COMITATO NAZIONALE PER L'ENERGIA NUCLEARE
Laboratori Nazionali di Frascati

LNF-72/75
21 Settembre 1972

H.C. Dehne, M. Preger, S. Tazzari and G. Vignola : LUMINOSITY MEASUREMENTS AT ADONE USING SINGLE AND DOUBLE BREMSSTRAHLUNG. -

Servizio Documentazione
dei Laboratori Nazionali di Frascati del CNEN
Casella Postale 70 - Frascati (Roma)

Laboratori Nazionali di Frascati del CNEN
Servizio Documentazione

LNF-72/75
21 Settembre

H. C. Dehne(x), M. Preger, S. Tazzari and G. Vignola: LUMINOSITY MEASUREMENTS AT ADONE USING SINGLE AND DOUBLE BREMSSTRAHLUNG. -

ABSTRACT. -

We report on the latest set of luminosity measurements carried out at Adone last March. Single (SB) and double (DB) bremsstrahlung reactions were measured at several energies and compared with the results obtained. at the same time, by the " $\mu - \pi$ " group, measuring small-angle-Bhabha-scattering. The three luminosity measurements were found to be in agreement within the expected systematic errors.

1. - EXPERIMENTAL SET-UP. -

Our apparatus is very simple, consisting mainly of three lead--scintillator sandwiches, and three plastic scintillators, arranged as shown in Fig. 1(o).

A1, A2, A3 are anticoincidence scintillator counters, while SW1, SW2, SW3 are the sandwiches. Two windows are provided in the vacuum

---

(x) - Now at DESY, Hamburg.

(o) - For details on cross-sections, signal-to-background ratios, angular distributions etc. refer to Ref. (1). The pressure in the ring, at the time of the measurements, was in the range of 10^{-9} Torr, and circulating currents were in the range of $10 \div 30$ mA per beam.

chamber, one at each side of straight section 11, while there is no window at straight section 8.

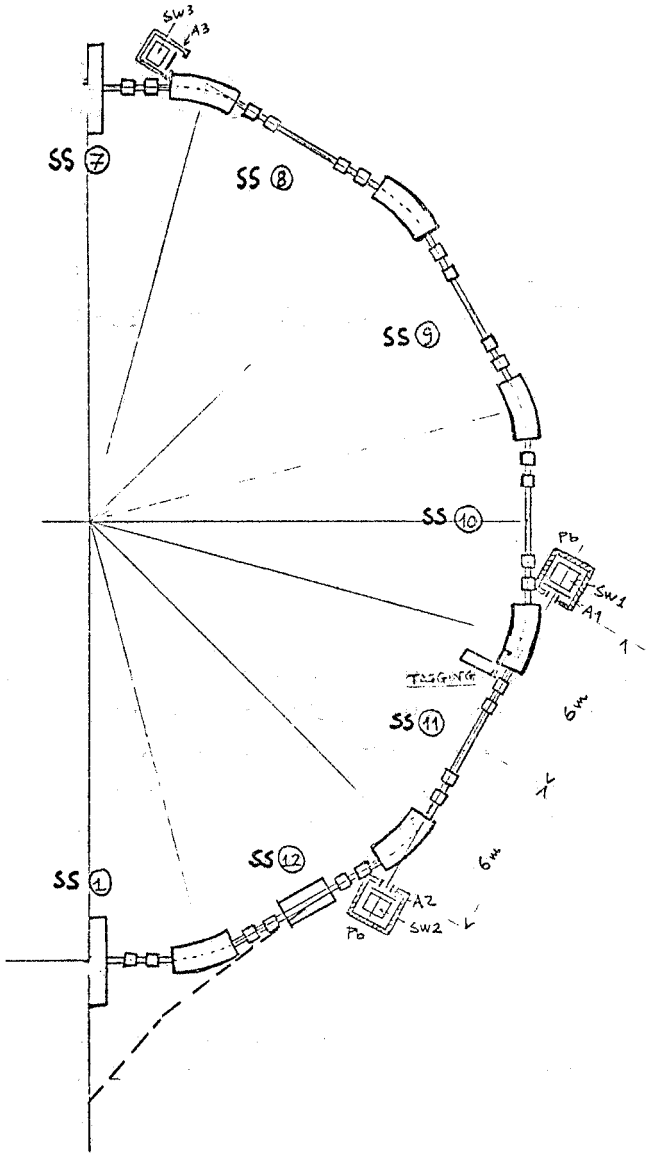

FIG. 1 - Experimental layout.

Unfortunately, the original 0.1 mm stainless-steel windows had to be taken out because of synchrotron-radiation heat problems, and were replaced by 3 mm-thick stainless-steel ones.

An additional counter, placed inside the magnet and projecting inside the vacuum chamber, has been occasionally used for tagging purposes. Sandwich counters 1 and 2 are built as shown in Fig. 2. They are linear up to 1500 MeV and their measured resolution is

(1) $$R = \frac{\Delta E}{E} \simeq \Gamma \left(\frac{E_{GeV}}{0.4}\right)^{-1/2} \qquad \Gamma = 0.35$$

In front of SW1 and SW2 there are two lead collimators defining a half--aperture angle, as seen from the center of the straight section, of 6 mrad.

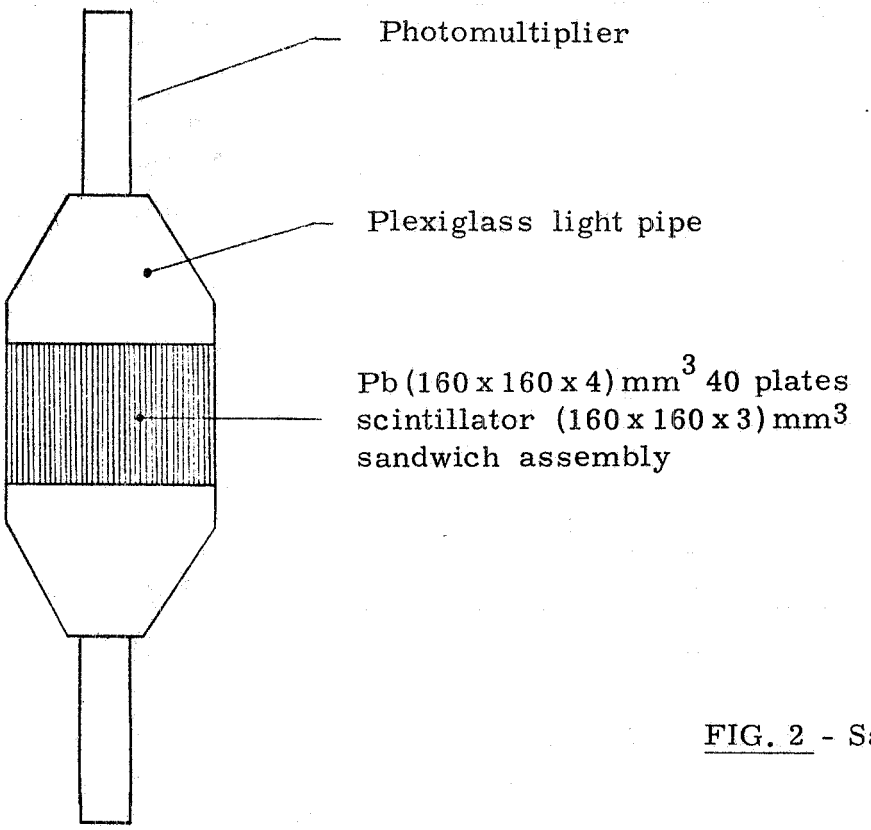

FIG. 2 - Sandwich counter.

Fig. 3 shows a simplified block diagram of the logics. SW3 is used for separating background from single bremsstrahlung events, as explained in detail in the following, and does not appear in the diagram.

Counters SW1 and SW2 were aligned with respect to the beam by looking at the outcoming γ-ray-beam profiles at the counters. Alignment is accurate to ± 0.2 mm both radially and vertically.

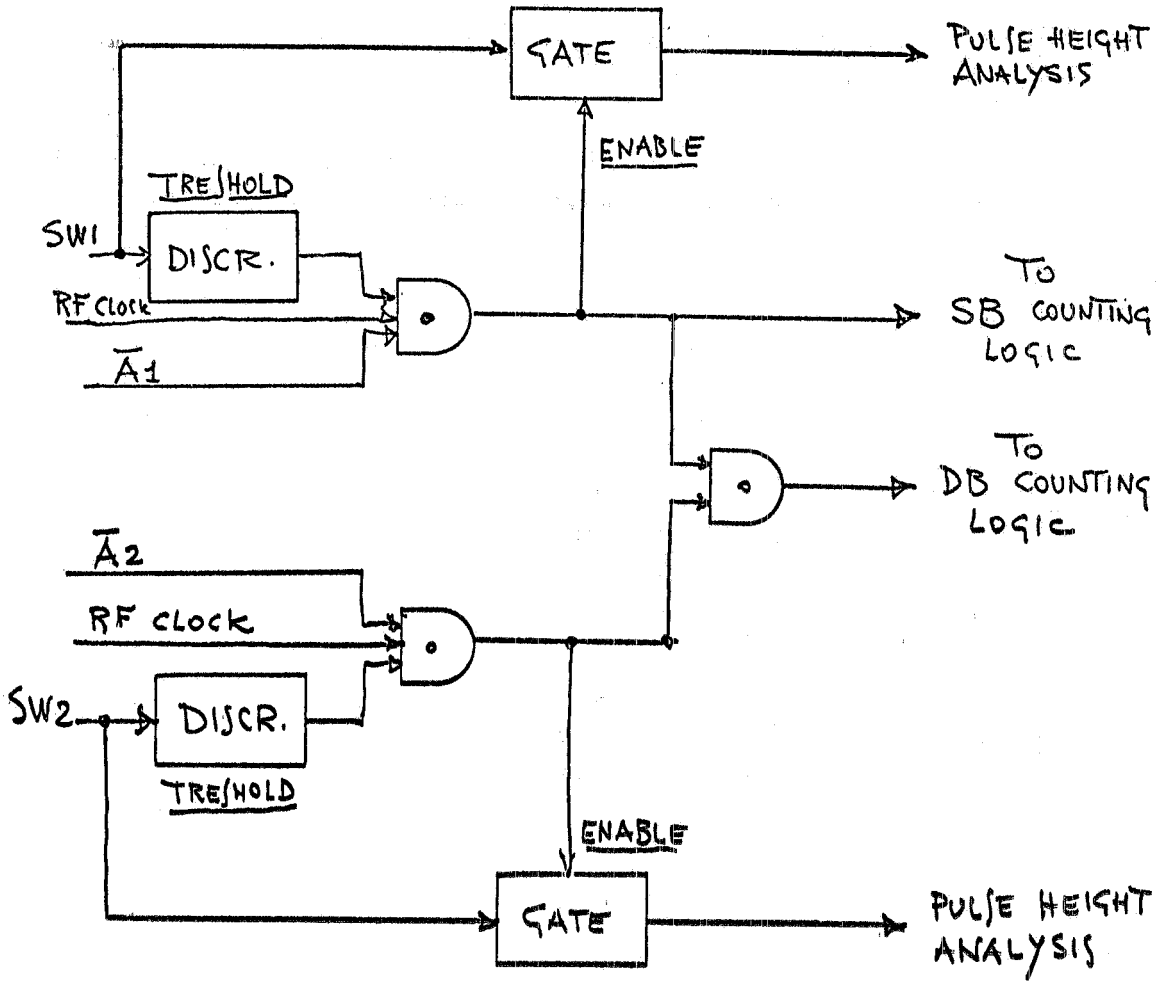

FIG. 3 - Simplified diagram of the logics for defining an event.

2. - BACKGROUND SUBTRACTION. -

a) - Single bremsstrahlung. -

As discussed in Ref. (1) the main source of background to this reaction is bremsstrahlung on the residual gas (GB).

The signal-to-background ratio can easily be as low as 10% so that subtraction requires special care and will be described in some detail. Let us, for convenience, assume that our counters face the e^+ beam. The event rate due to bunch i at interaction straight section k is given by

$$\dot{n}_i^k = G_i^k N_i^+ + \S L_i^k (N_i^+, N_j^-) \qquad i, k = 1, 2, 3 \tag{2}$$

where $N_i^{\pm}$ is the number of $e^{\pm}$ in bunch i and $L_i^k(N_i^+, N_j^-)$ is the luminosity produced by the crossing, in k, of bunch i of the e^+ beam with bunch j of the e^- beam. G_i^k and S are coefficients.

G_i^k, the background yield per circulating particle, is given by:

$$(3) \qquad G_i^k = (\alpha Z_{AV}^2 P \frac{\nu_{RF}}{k} l) \int_\varepsilon^1 \int_\Omega (\frac{d^2\sigma_{GB}(\varepsilon)}{d\varepsilon\, d\Omega} d\varepsilon\, d\Omega)_i^k + F_i^k$$

where:

α = 3.55×10^{-16} cm^{-3}

Z_{AV}^2 = average quadratic value of the atomic number of the residual gas

P = pressure of the residual gas (torr.)

ν_{RF}/k = revolution frequency = 2.86×10^6 s^{-1}

l = lenght of straight section = 6.1 m

$d^2\sigma_{GB}(\varepsilon)$ = differential gas-bremsstrahlung cross-section

ε = fractional γ-ray energy = $E\gamma/E_{MAX}$.

All parameters appearing in (3) could depend on k, and a dependence on i of some of them need not be excluded. We have therefore labeled G with two indexes i, k. The first term on the right hand side of eq. (3) is the dominant one and is due to GB, while F_i^k is the contribution of all other backgrounds proportional to N_i, such as γ-rays from electrons lost on the vacuum chamber walls and the like.

S is given by:

$$(4) \qquad S = \int_\varepsilon^1 \int_\Omega \frac{d^2\sigma_{SB}(\varepsilon)}{d\varepsilon\, d\Omega} d\varepsilon\, d\Omega$$

and is calculated in ref. (1).

The quantity to be measured with great accuracy is therefore $G_i^k N_i$ or rather its average value over the time interval necessary to perform the luminosity measurement.

The way the average $G_i^k N_i$ has been measured can best be explained by assuming at first that only two bunches of positrons (1^+, 2^+) and one of electrons (1^-) are present, and recalling that we have two counters, one facing an interaction straight section (SW1 at straight section 11), and the other facing a non-interaction straight section (SW3 at straight section 8).

The positron bunch 1^+ will collide, at straight section 11, with the electron bunch 1^-, while bunch 2^+ will have no corresponding e^- bunch to collide with. At straight section 8 (a non-interaction straight section) neither e^+ bunch will undergo a collision.

The counting rate of bunch 2^+ at straight section 11 will therefore be due to background only, yielding a measurement of $G_2^1 N_2$, while the counting rates of SW3 will yield an accurate value of the ratio $G_2^2 N_2^+ / G_1^2 N_1^+$. We have

$$(5) \qquad \begin{cases} \dot{n}_1^1 = G_1^1 N_1^+ + S L_1^1 (N_1^+, N_1^-) \\ \dot{n}_2^1 = G_2^1 N_2^+ \\ \dot{n}_1^2 = G_1^2 N_1^+ \\ \dot{n}_2^2 = G_2^2 N_2^+ \end{cases}$$

From (5) one obtains

$$S L_1^1 (N_1^+, N_1^-) = \left(\frac{\dot{n}_1^1}{\dot{n}_2^1} - \frac{G_1^1 N_1^+}{G_2^1 N_2^+} \right) \dot{n}_2^1$$

We now make our first assumption, namely:

$$(6) \qquad \frac{G_1^1}{G_2^1} = \frac{G_1^2}{G_2^2}$$

Under this assumption

$$(7) \qquad S L_1^1 (N_1^+, N_1^-) = \dot{n}_1^1 - \frac{\dot{n}_1^2}{\dot{n}_2^2} \dot{n}_2^1$$

where all quantities on the right hand side are measured with very small statistical errors, the counting rate being high. Failure of assumption (6) must be envisaged as a possible source of errors. The method can be straightforwadly extended to the case where three e^+ bunches and two e^- bunches are present, if the third e^- bucket is

completely empty. Actually a measurement of L can be made, provided only the current of at least one e^- bunch is not identical to that of the others, under one further assumption, namely that L be a function of the product of the currents of the colliding bunches only:

$$L = \text{const} \times (N_i^+ N_j^-) \tag{8}$$

Of course, if the difference is too small, the statistical error is very large. We will come back to this point when dealing with the corrections made.

b) - Double bremsstrahlung. -

In this case, the events being defined by a double coincidence, background subtraction can be made with the usual delayed coincidence technique, provided only the delay is equal to one full machine revolution.

3. - THRESHOLDS. -

The next major problem in connecting counting rates to luminosity is that of determining the exact value of the threshold energy for γ-ray detection.

We recall that

$$\dot{n}_\gamma \propto L \int_{E_{th}}^{E_{MAX}} \frac{d\sigma}{dE}(E)\, dE$$

where $d\sigma/dE\,(E)$ is the differential single (or double) bremsstrahlung cross section. The value of E_{th} is of course determined by the setting of the discriminators (see Fig. 3).

E_{th} can be found by calibrating the GB pulse-height spectra

a) against the theoretical ones, the machine energy being well known,
b) against a tagged spectrum of known energy.

After checking that results obtained through the two methods were in good agreement, we chose to rely, during normal operation, on method a) which is more practical.

a) - Energy calibration by means of the high energy cut in the GB spectrum.-

The thin target energy spectrum of γ-rays from GB, in the extreme relativistic case and for complete screening, can be found in Ref. (2) and Ref. (3).

Since the spectrum does not change with energy if the reduced variable $\varepsilon = E_\gamma / E_{MAX}$ is used, we have plotted in Fig. 4 the product of ε times the spectral function $n(\varepsilon)$, versus ε.

Given the energy resolution of our counters (see formula (1)), the curves of Fig. 4 are obtained by folding R into the theoretical spectrum for different values of Γ.

It can be seen that, since the high energy part of the GB spectrum is, in the approximations of Ref. (2) and Ref. (3) a step function, all curves with $\Gamma \neq 0$ cross the $\varepsilon = 1$ step at almost exactly the same point, no matter what the value of Γ (at least for $\Gamma \leq 0.6$).

Moreover all spectra have a nearly flat region at around $\varepsilon \approx 0.65$, so that the following approximate method for finding channel C_M, corresponding to $\varepsilon = 1$ in our pulse height spectrum, can be envisaged: assume y_P to be the ordinate of the flat region (plateau) of the spectrum, C_M is then the abscissa of the point on the spectrum, which has the ordinate

$$y_M = \frac{y_P}{1.82\,(1 \pm 0.013)}$$

The introduction of a more sophisticated shape for the high energy side of the bremsstrahlung spectrum (Ref. (2) and (3)) leads to corrections that are small with respect to the overall accuracy of our reconstruction of spectra, and were therefore neglected.

We also need to know what channel (C_o) in our pulse height spectrum corresponds to zero-energy. By knowing C_o and C_M, and assuming the pulse height analysis chain is linear, we have an energy calibration of the apparatus, and can therefore proceed to find E_{th}.

Let us briefly describe how the actual system works: counter pulses enter a linear gate, are superimposed on a constant amplitude pedestal, and are then fed to a 200-channel pulse height analyzer. An external clock continuously generates "pedestal-only" pulses, which are also fed, during the measurement, to the analyzer. The zero-energy channel C_o can thus be identified on each spectrum. Once a spectrum is completed, it gets directly transferred to a computer, which identifies C_o and C_M, calculates the calibration factor

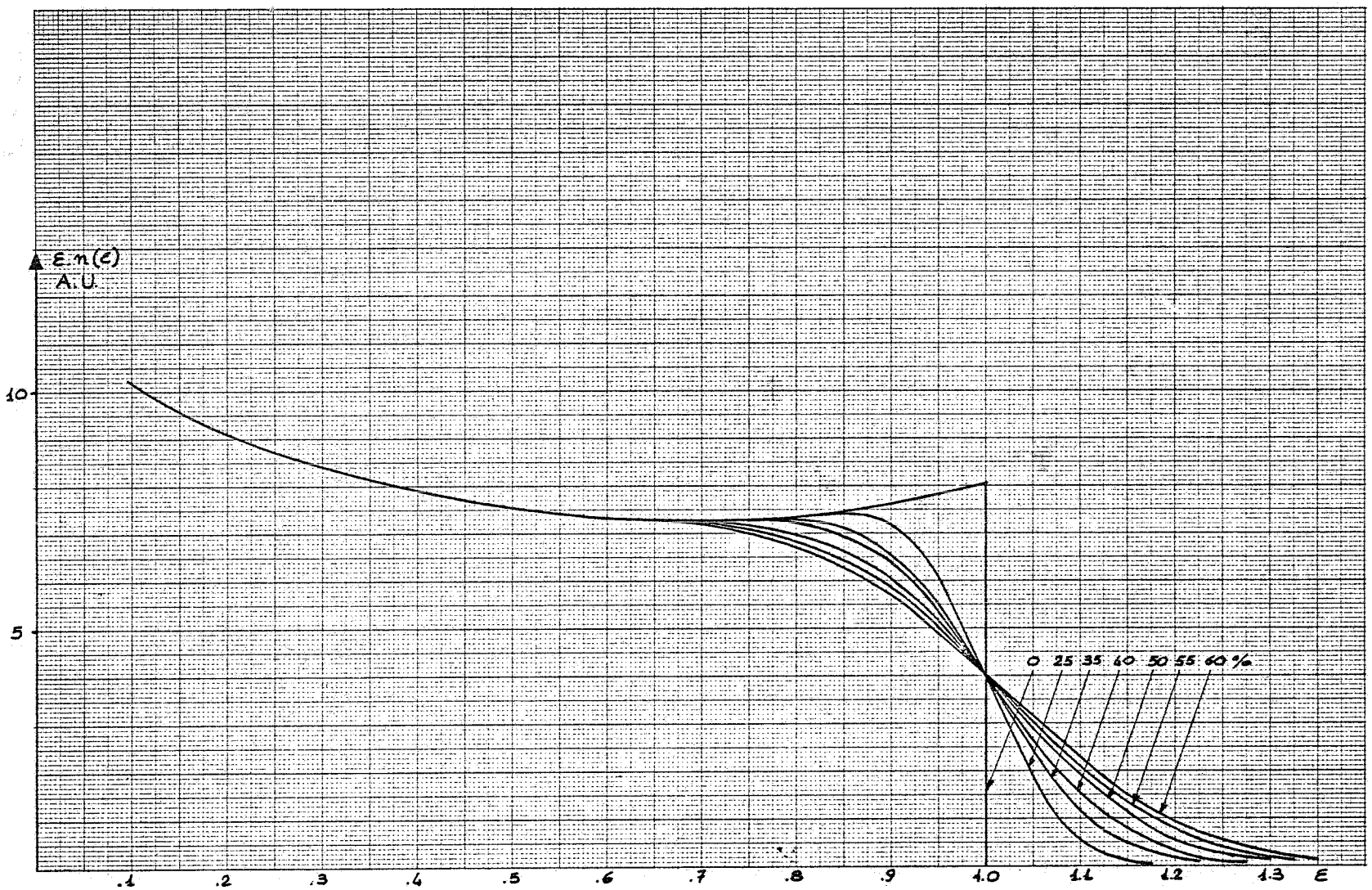

FIG. 4 - Differential gas-bremsstrahlung spectrum at a maximum energy of 1000 MeV, with resolutions: $\Delta E/E = 0$, 25, 35, 40, 50, 55, 60% at 400 MeV.

$$f = \frac{E_M}{C_M - C_o}$$

which is the width of a channel in energy units, and compares the shapes of the experimental and theoretical spectra, by normalizing one to the other at one point (on the plateau).

Fig. 5 explains how the threshold energy is defined, by equating the areas under the two spectra.

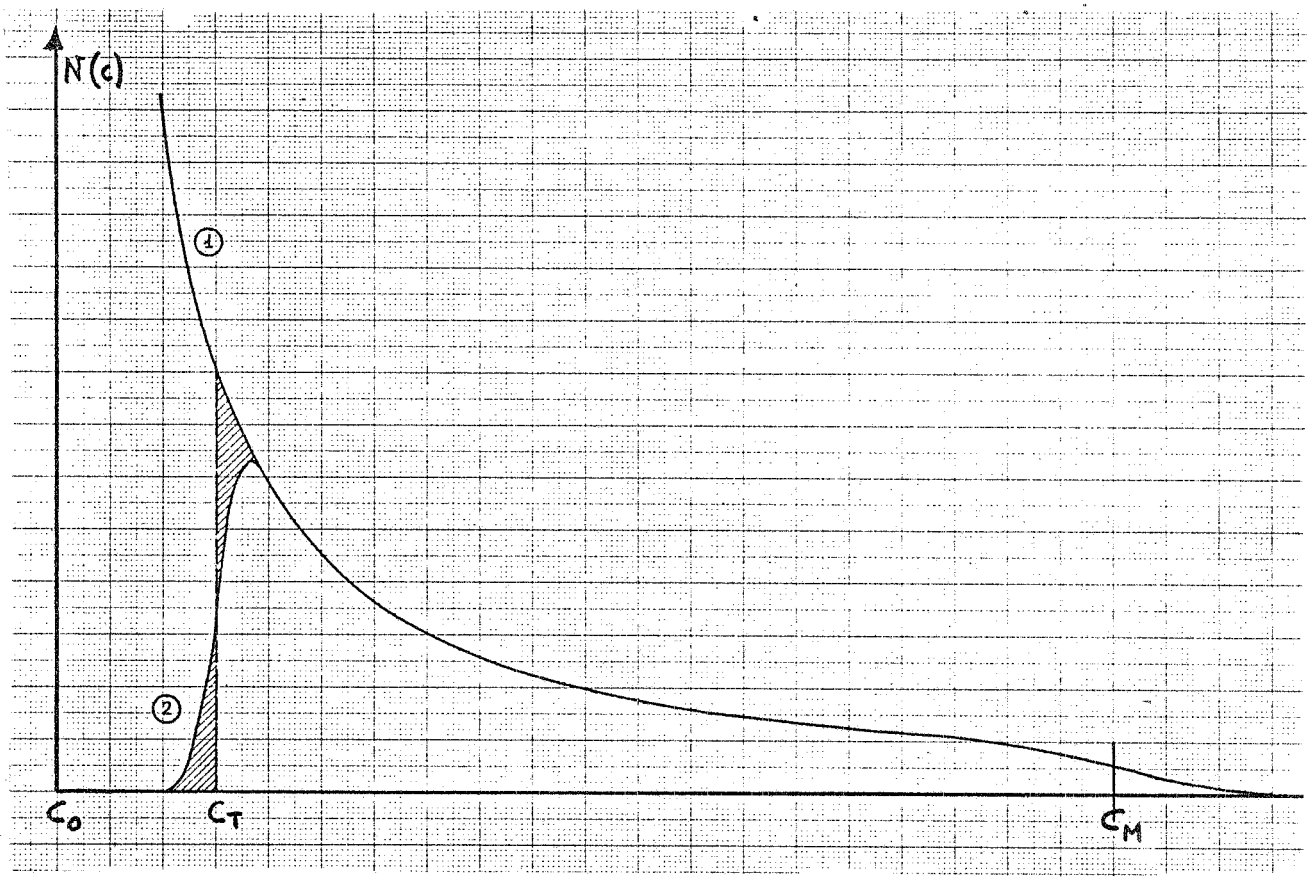

FIG. 5 - Method for finding the threshold. Curve (1) is the theoretical spectrum, while curve (2) is the experimental one. C_T is defined by the condition that the two dashed areas be equal. E_T is given by:

$$E_T = (C_T - C_o) f = (C_T - C_o) \frac{E_M}{(C_M - C_o)}$$

We will come back on this subject when discussing the measurements.

b) - Tagging. -

A small ($1 \times 1 \times 1$ cm^3) plastic scintillator counter was installed inside one of the magnets adjacent to straight section 11 (see Fig. 1). The two quadrupoles and part of the magnet act as a momentum analyzer for electrons accompanying bremsstrahlung γ's. The γ and the accompanying electron (of known energy) can thus be detected in coincidence. If the accepted electron momentum-byte is small enough, the associated γ's are quasi-monochromatic.

Our counter was placed at (6 ± 0.06) magnetic degrees inside the magnet, at a distance of (12 ± 1) cm from the equilibrium orbit. Taking into account the closed orbit position and angle, the peak of the γ-ray energy distribution was calculated to be at

$$\varepsilon = 0.85 \pm 0.01$$

The error quoted is a mean square standard deviation. Fig. 6 shows one of the measured peaks. The test was performed at 1 GeV. The width of the peak corresponds to the 850 MeV resolution of the sandwich, since the resolution of the tagging system ($\Delta p/p \approx 3\%$ fwhh) is much better than that of the counter (24% fwhh). The calculated position of the peak agrees, well within the errors, with that estimated using method a).

4. - PERFORMANCE OF THE APPARATUS. -

Several tests were performed, both before and during the experimental runs, to check on the performance of the apparatus.

We mainly had to check the accuracy of the subtraction procedure (both for single and for double bremsstrahlung (SB and DB)) and the linearity of the pulse height analysis.

a) - Background subtraction. -

Before running, it was checked that, with one beam only and under all machine operating conditions, the ratios between the counting rates due to the three different bunches, $\dot{n}_i/\dot{n}_{i+1}$, measured in section 11, were the same as those measured in section 8. The agreement was found to be within the statistical errors (a few tenths of a percent). This is of course a test of hypothesis (6) of § 2. Hypothesis (8) can only be checked indirectly (see § 6, b)).

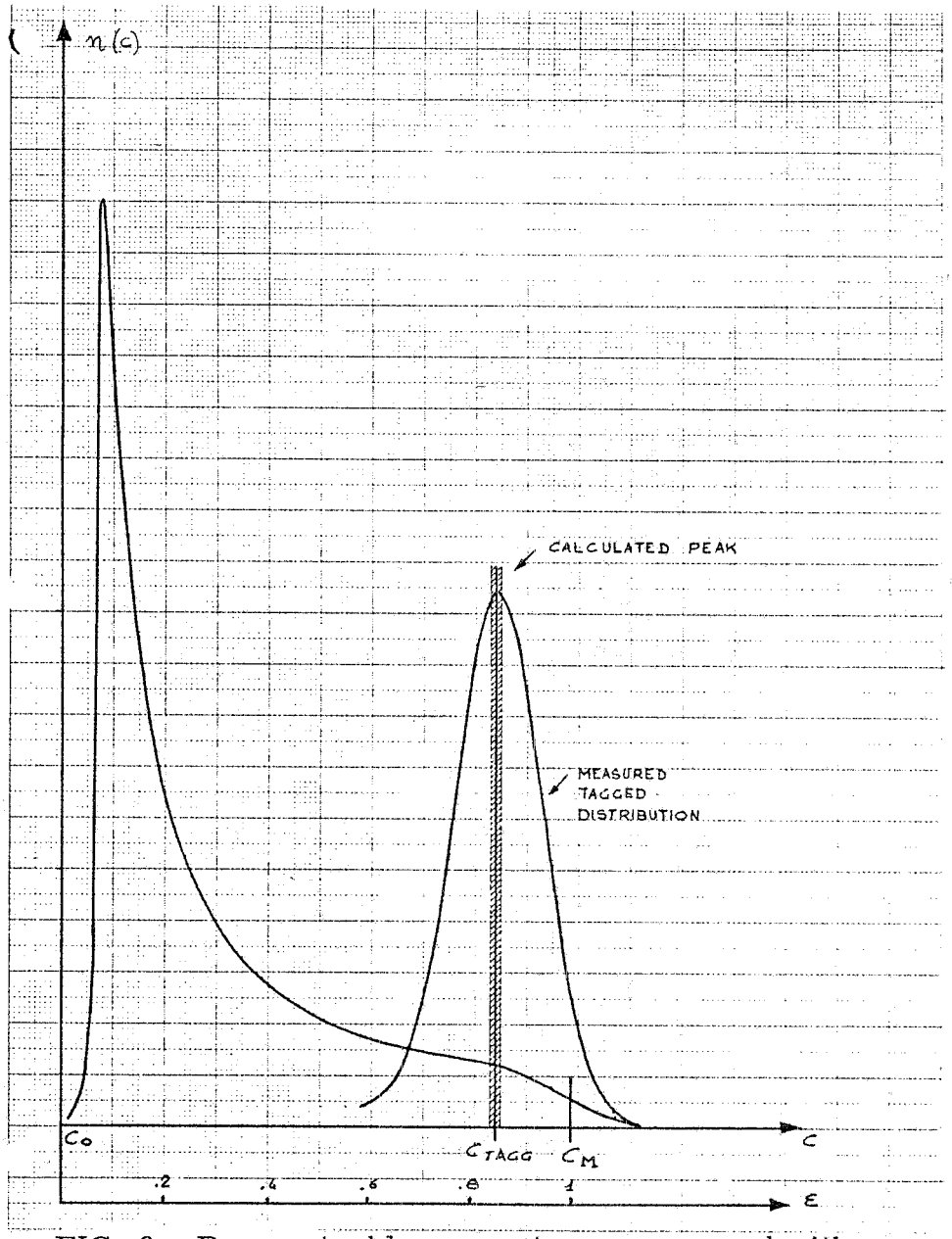

FIG. 6 - Bremsstrahlung spectrum compared with tagged spectrum (amplified).

An overall test of the correctness of the procedure is the measurement of SB and DB luminosity with two vertically separated beams. A collection of these "background" measurement, performed over several days during the experimental runs, is shown in Fig. 7 and Fig. 8. We plot the ratio of luminosity measured with vertically separated beams to that measured with crossing beams. In the case of DB (see Fig. 8) the set of all measurements shows the "background" luminosity to be zero, within the errors, independent of energy. The χ^2 value of the distribution is 34.9 against an expected value of (37 ± 9). The measured luminosities need not therefore be corrected.

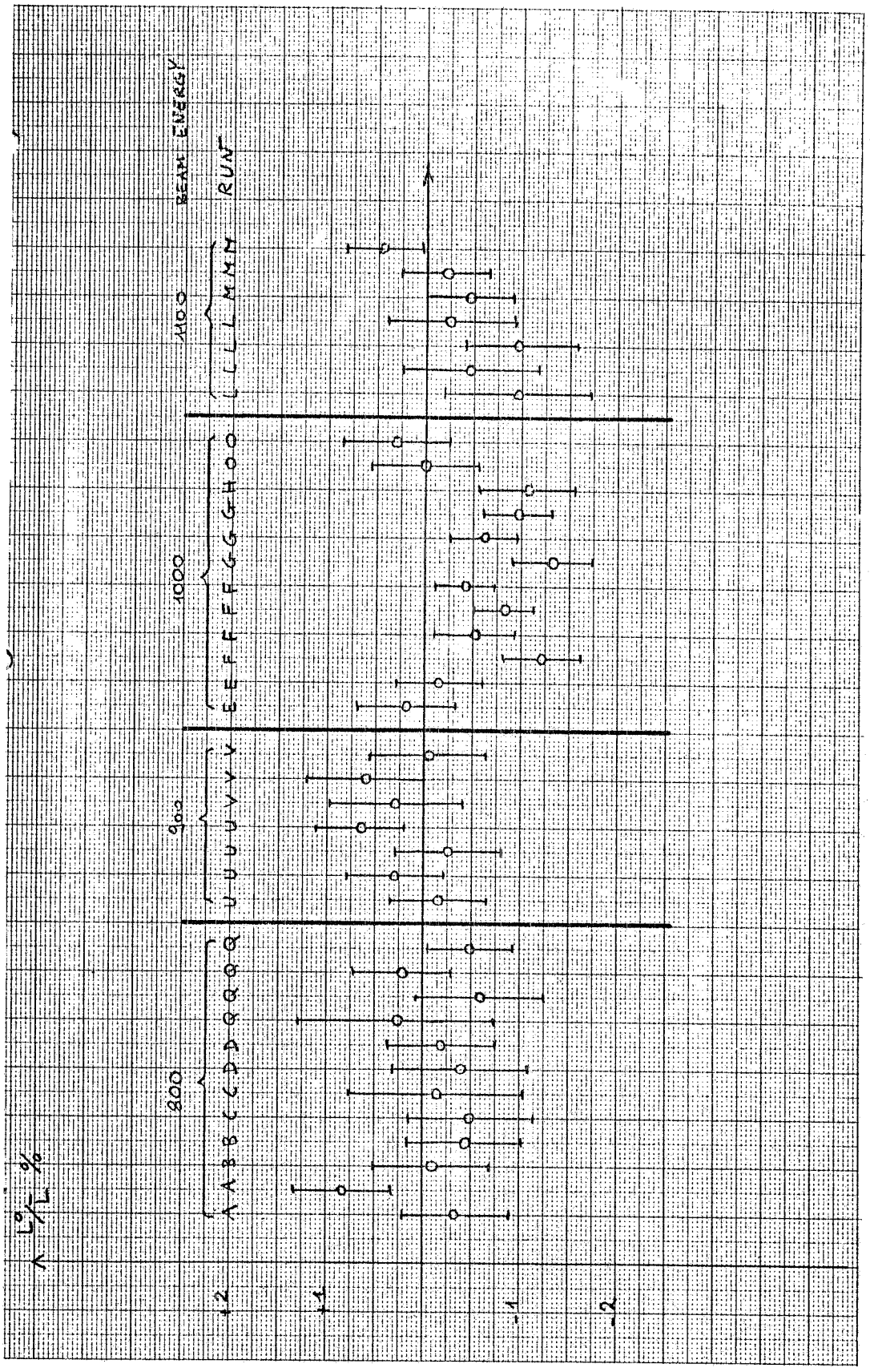

FIG. 7 - Separated beams "background" luminosity. Single bremsstrahlung.

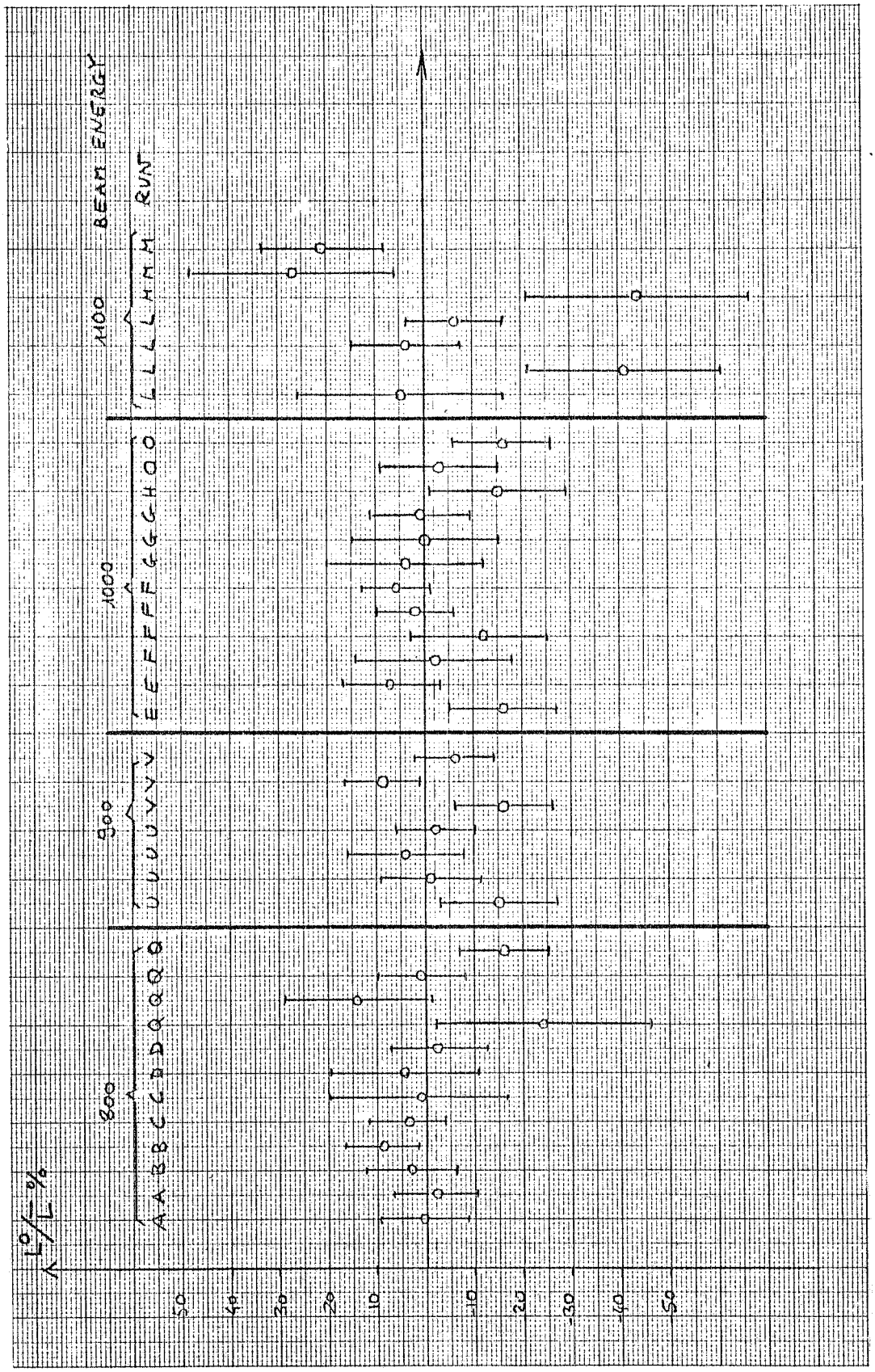

FIG. 8 - Separated beams "background" luminosity. Double bremsstrahlung.

The situation is somewhat more complicated in the case of SB (see Fig. 7). The points are distributed around an "average" value of (-0.35)%, the distribution having a χ^2 of 46 against an expected value of (37 $\pm$ 9). Moreover there seems to be a dependence on energy. The latter could in principle be expected since residual gas pressure, current, and machine conditions are widely different at different energies. However, the maximum deviation from the "average" being at all energies of $\pm$ 0.5%, (compatible with the errors on the above mentioned measurement of bunch-current ratios), we have taken the view of correcting all SB luminosity measurement by 0.35%, and of increasing by $\pm$ 0.5% their systematic error. Fig. 9 shows the behaviour of L_o/L as a function of the signal to background ratio. Note that in the case of SB, given our subtraction procedure and the low signal to background ratios, L_o is very sensitive to possible systematic errors on the measurement of the ratios between bunch currents.

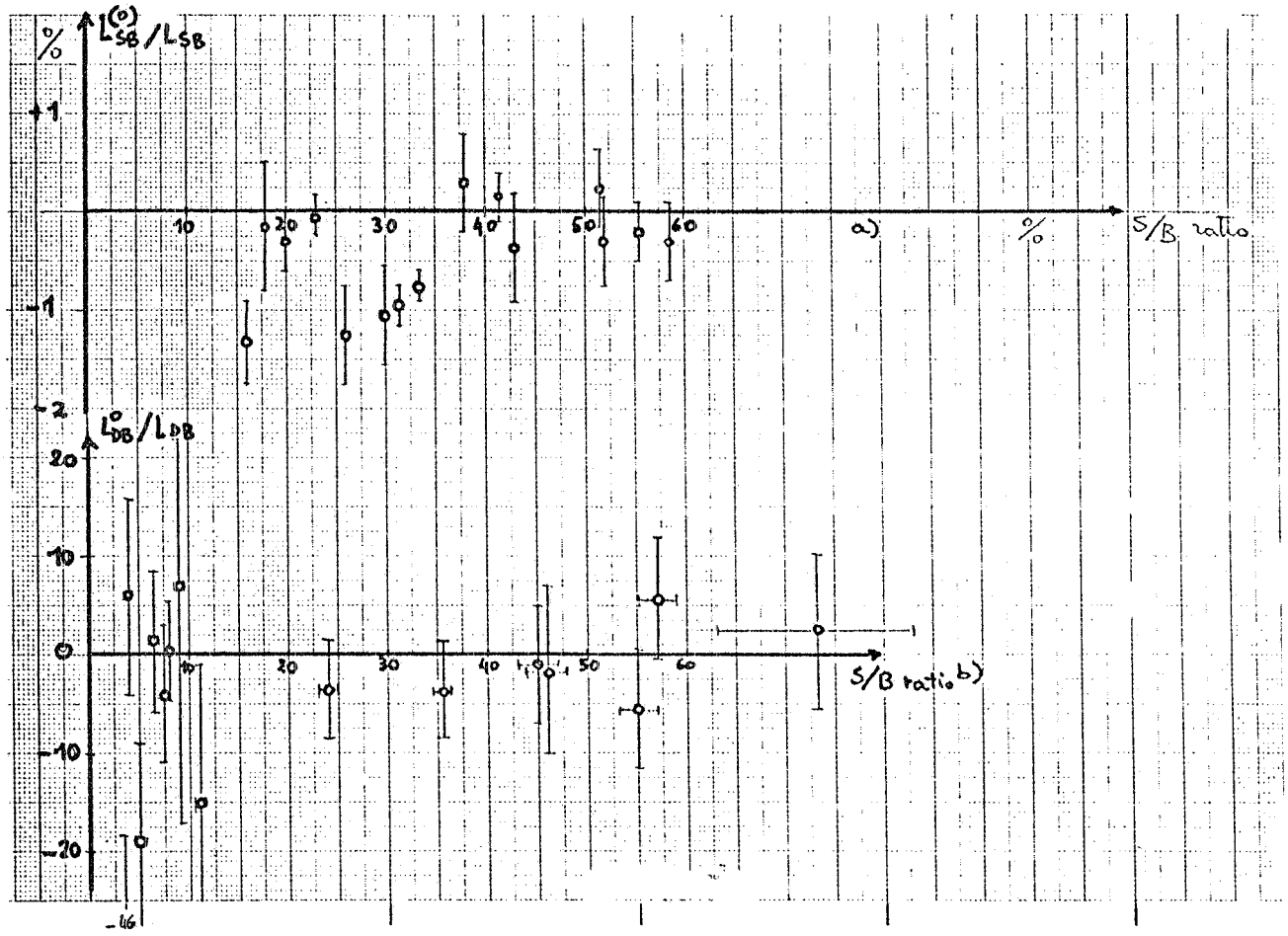

FIG. 9 - Separated beams "background" luminosity as a function of signal-to-background ratio. Single and double bremsstrahlung.

b) - Linearity of the pulse-height analysis chain.-

The sandwich counters were tested in a monoenergetic beam of 100÷700 MeV electrons. They were found to be linear within the experimental errors in this range, and the resolution was found to vary as the square root of energy, as expected, being ~ 35% fwhh at 400 MeV. More accurate tests of the whole chain were performed at the storage ring, using the bremsstrahlung beam.

The linearity of the electronics has been tested using a pulser. Differential and integral linearities have been found to be within ± 0.3 channels, which is compatible with the pulse-height analyzer specifications.

Fig. 10 shows the linearity of SW1 and SW2 versus energy. The dots in Fig. 10 are values obtained for C_{MAX}, using our analyzing program. The crosses are points obtained by subtracting spectra of the same series one from the other. This leaves of course a peak of quasi-monochromatic γ's. We plot the peak-channel position.

A best fit of the points with a straight line gives an error on the extrapolated zero-energy position of (-0.12 ± 0.3) channels for SW1.

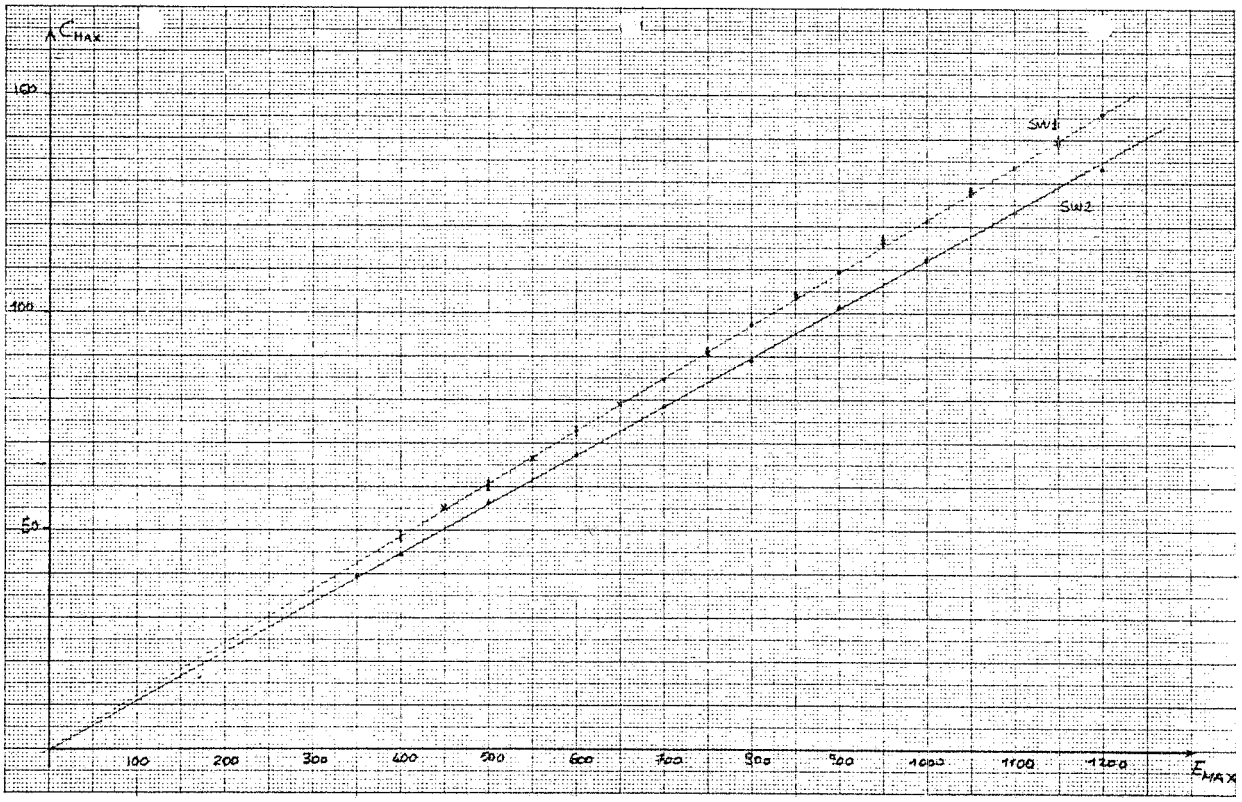

FIG. 10 - Linearity of pulse-height analysis chains.

SW2 is slightly worse, since the phototube shows a beginning of saturation at around 1200 MeV. The extrapolated zero-energy position, obtained fitting the points in the interval from 350 to 1100 MeV, is however (0.06 ± 0.4) channels.

5. - EXPERIMENTAL BREMSSTRAHLUNG SPECTRA. -

a) - Gas Bremsstrahlung. -

Our method for determining the detection threshold requires the gas bremsstrahlung spectra of both counters to be analyzed.

A typical spectrum, obtained during an experimental run at the energy of 1000 MeV is shown in Fig. 11 for SW1 and in Fig. 12 for SW2, superimposed on the theoretical spectrum. A slight discrepancy between theoretical and experimental shapes can be observed, its magnitude being slightly lower for SW2 than for SW1. The ratio:

$$\frac{\left[\varepsilon\, n(\varepsilon)\right]_{th} - \left[\varepsilon\, n(\varepsilon)\right]_{exp}}{\left[\varepsilon\, n(\varepsilon)\right]_{th}}$$

is negative, but never exceeding $\sim 3\%$ at the lowest end of the spectrum. Such an effect could of course be due mainly:

a) to a non-linearity of our analyzing chain or of our counters,
b) to a physical effect causing a slight energy degrading of the spectrum.

The effect has been studied with some care and the tentative conclusion we reach is that there is at least some background of low energy γ's produced inside the vacuum chamber(x). Should the effect be due to a non-linearity of our system alone, it would be just barely compatible with our estimated maximum errors.

Reflections of this discrepancy on our threshold values will be discussed in the paragraph on experimental errors.

b) - Single beam-beam bremsstrahlung. -

The bunch configuration used during the measurements, having one e^- empty bucket, allows the beam-beam single bremsstrahlung spectrum to be extracted, on a statistical basis, from a spectrum containing both GB and SB.

(x) - We could not however prove this point through direct measurements.

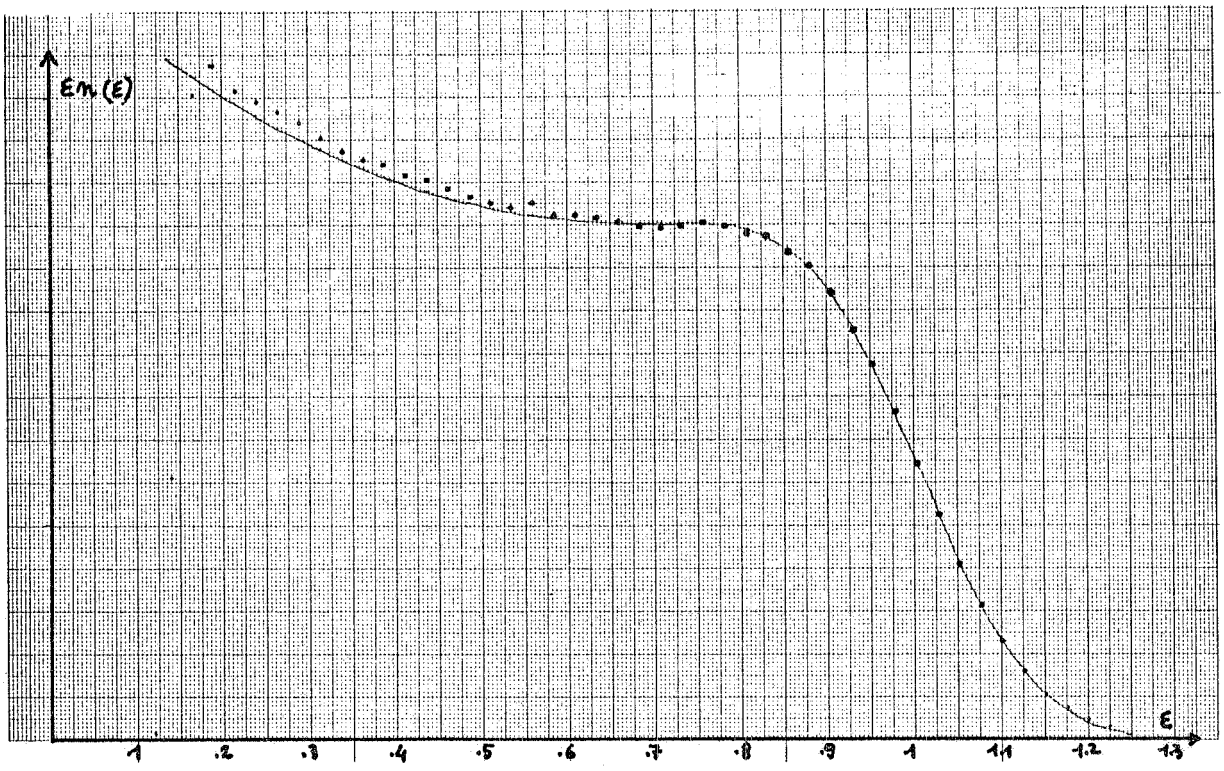

FIG. 11 - Experimental gas-bremsstrahlung spectrum compared with theoretical spectrum - SW1 - Beam energy 1000 MeV.

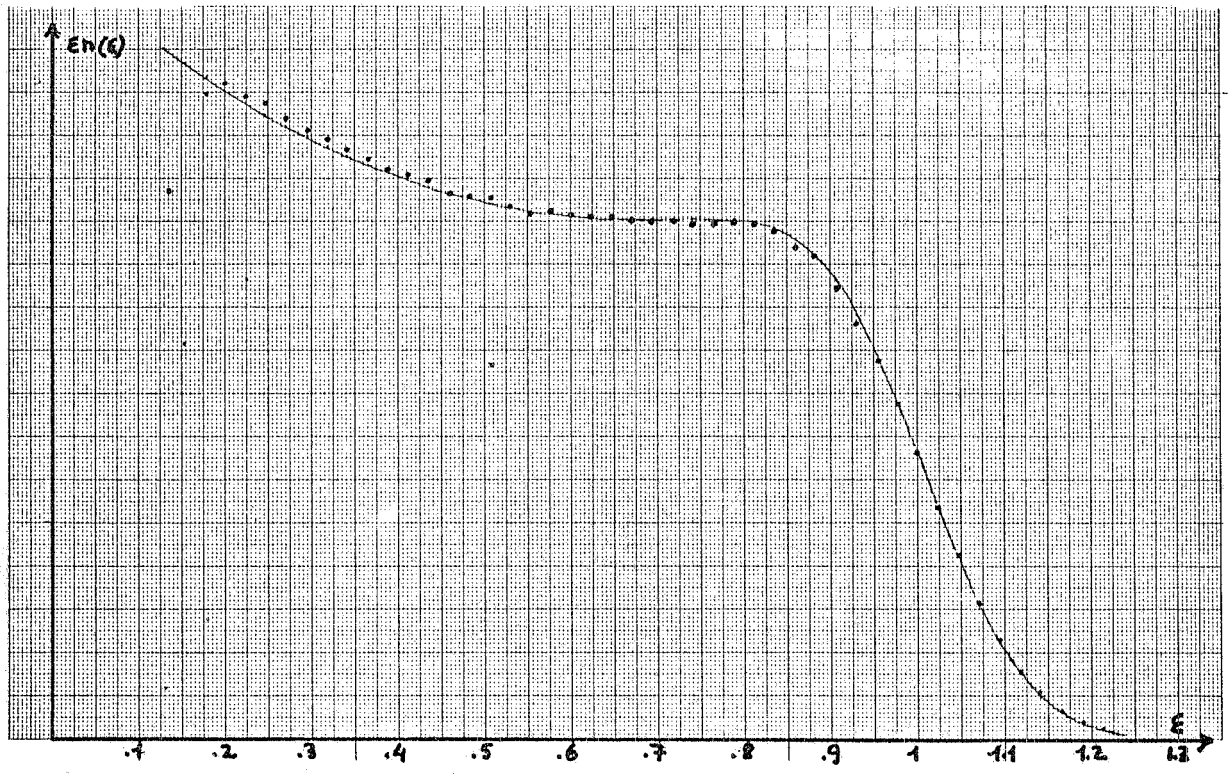

FIG. 12 - Experimental gas-bremsstrahlung spectrum compared with theoretical spectrum - SW2 - Beam energy 1000 MeV.

During the same run, the spectrum due to the e^+ bunch "colliding" with the empty e^- bucket, which is a pure GB spectrum, can be collected, normalized with the ratio of the currents (which we measure with great accuracy (see § 2)) and subtracted out from the total spectrum. A spectrum obtained in this way is shown in Fig. 13 superimposed on the theoretical shape. The agreement is seen to be better than that of gas bremsstrahlung spectra, although it is not perfect. The residual discrepancy (of the order of 2% at the lowest end) is well within our "linearity" errors, and could also be in part attributed to a slight, uncorrected-for energy degradation in the thick window (see § 6). A quantitative estimate of this last effect is rather difficult to obtain, and, the residual discrepancy being compatible with our estimated systematic errors, the effect was neglected. The fact that SB spectra agree with the calculated shape better than GB spectra seems to support our previous conclusion that at least part of the effect is due to a background originating inside the vacuum chamber, which would of course be subtracted out from the beam-beam SB spectrum.

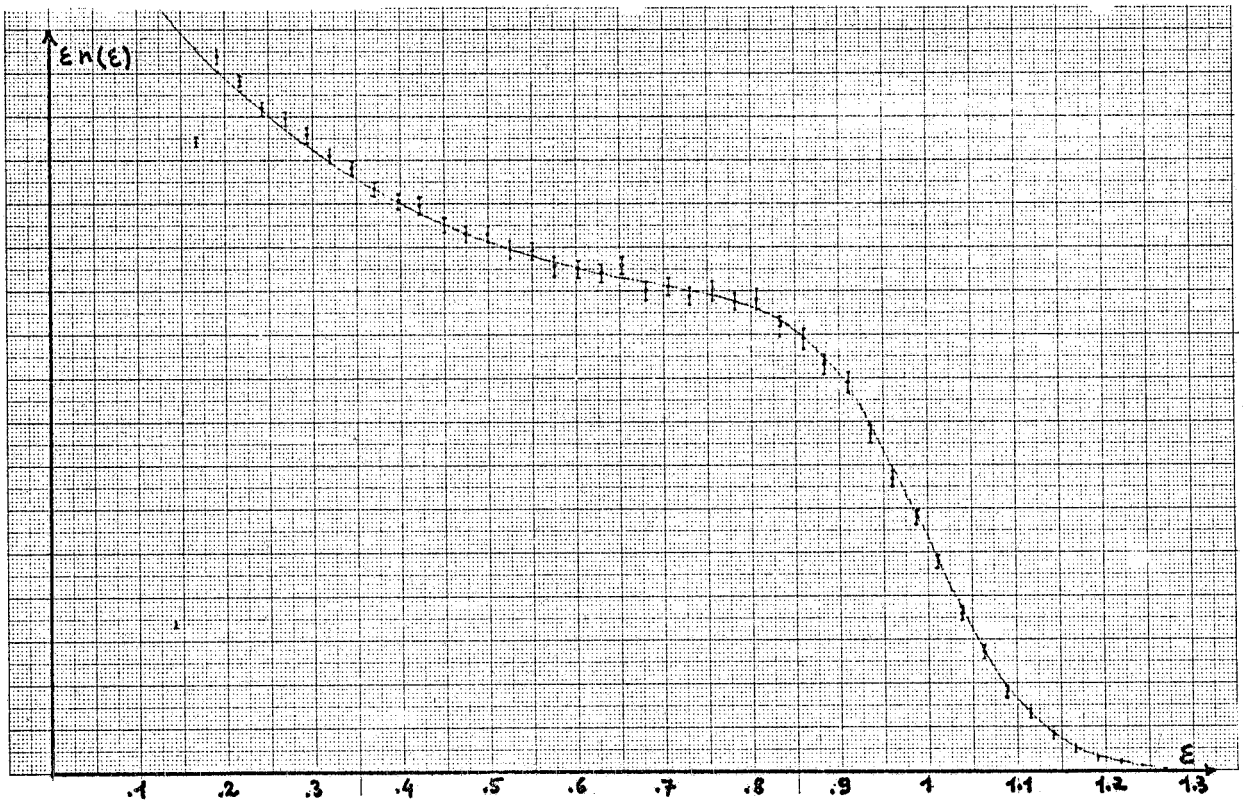

FIG. 13 - Experimental single-bremsstrahlung spectrum compared with theoretical spectrum - SW1 - Beam energy 1000 MeV.

6. - CORRECTIONS. -

a) - Conversions in the thick window. -

The γ-rays we detect have gone through a 3 mm stainless steel flange situated inside the fringing field of one of the machine bending magnets. The latter acts, at least in part, as a clearing field. We require, however, in order to have a clean spectrum, counters A1 and A2 (see Fig. 1) to be in anticoincidence.

Our event rate has therefore to be corrected for conversions in the flange and in counters A1 and A2. A small residual contamination of degraded γ's having converted in the flange (or elsewhere) but going through A without firing it, remains. Their number has been measured and is given by $\dot{n}_s \, \delta_3$, where $\dot{n}_s$ is the rate of RF. SW. $\bar{A}$ counts, and $\delta_3 = (1 \mp 0.2)\%$, independent of machine conditions.

Conversions in a flange identical to that mounted on the machine, and in the anticoincidence counter have been measured too.

The overall correcting factor for SB is:

$$f_{SB} = \frac{1}{1-(\delta_1 + \delta_2 - \delta_3)}$$

where $(\delta_1 + \delta_2)$ is the fraction of γ's, which converts in the flange and in the anticoincidence counter.

We have measured

$$(\delta_1 + \delta_2) = (12.7 \pm 0.2)\%, \qquad \delta_2 = (2.5 \pm 0.2)\%$$

so that we have

$$f_{SB} = (1.133 \pm 0.005)$$

For double bremsstrahlung (A2 is slightly thicker than A1) we have measured:

$$f_{DB} = (1.295 \pm 0.012)$$

The calculated value for δ_1 is 10.5%, in good agreement with the measured value.

b) - Residual bunch.-

Our assumption that one e^- bunch is completely empty is not in practice always true. It is however possible to correct the measured luminosity value for the effect due to the residual current in the bunch. Assuming bunch 3^- is the "empty" one, the correction factor is given by

$$f_i = \frac{\beta_2 + \alpha_3 + \alpha_2 \beta_3}{(\beta_2 - \beta_3) + \alpha_3(1 - \beta_3)}$$

$$\alpha_k = i_k^+ / i_1^+ \qquad \beta_k = i_k^- / i_1^- \qquad k = 2, 3$$

The factors α_k and β_k are carefully measured with vertically separated beams.

The hypotheses made are that the coefficients relating SB and GB to counting rates are the same for the three pairs of crossing bunches, notwithstanding the large difference in the product of currents; the proof of the correctness of the hypothesis lies, in our opinion, in the fact that, while f_i ranges for our measurements in between 1.00 and 1.18, no dependence of the results on f_i has been observed (see § 8 Fig. 17). This correction applies of course to SB only, so that agreement between SB and DB luminosity is a further check on the above assumptions.

c) - "Background" luminosity correction.-

As discussed in § 4, no correction for "background" luminosity has been applied to DB data.

SB data were instead corrected by the factor

$$f_{BL}^{SB} = 1.0035 \pm 0.005$$

The error takes into account uncertainties in the "background" luminosity correction which can be attributed to differences in the background subtraction error between different points, due to different machine conditions.

7. - ERRORS. -

Luminosity is given by the general formula

$$L = \frac{\dot{n}_{(S+B)} - \dot{n}_B}{\sigma} \tag{9}$$

where $\dot{n}_{(S+B)}$ is the signal+background counting rate, $\dot{n}_B$ the background counting rate and σ the effective cross section of the process being observed.

a) - Single bremsstrahlung. -

As discussed in § 2, $\dot{n}_B$, the background counting rate, is given by

$$\dot{n}_B = \bar{\dot{n}}_B R$$

$\bar{\dot{n}}_B$ being the counting rate due to the e^+ bunch which interacts with the e^- empty bucket, and R being essentially an appropriate ratio of currents times factors of the type G_1^i/G_2^i (see § 2).

$\dot{n}_{(S+B)}$ and $\bar{\dot{n}}_B$ are measured by the same telescope, so that all possible drifts are the same for both.

Aside from statistical errors, the only source of errors on SB counting rate $(\dot{n}_{(S+B)} - \dot{n}_B)$ is term R. The best check on the magnitude of any systematic error in the subtraction procedure is the measurement of luminosity with vertically separated beams. The results have been presented in § 4. We have assumed a systematic deviation of -0.35% which has been corrected for (see § 6). The error on the deviation ($\pm$0.5%) will be added to the systematic errors on L.

The cross section appearing in the denominator of (9) is given by

$$\sigma_{SB} = \int_{\varepsilon_T}^{1} \int_{\Omega} \frac{d\sigma(\varepsilon, \theta, E_{MAX})}{d\varepsilon \, d\Omega} \, d\varepsilon \, d\Omega$$

ε_T and Ω are measured values, ε_T being the threshold energy and Ω the acceptance solid angle.

a1) Error on ε_T. -

Our method for evaluating ε_T was described in § 3. We have:

$$\varepsilon_T = \frac{E_T}{E_{MAX}} = \frac{C_T - C_o}{C_M - C_o}$$

C_T, C_o, C_M are affected both by random and by systematic errors. The random error on C_T, C_o and C_M is of the order of ± 0.1 channels at most. $(C_T - C_o)$ being of the order of 15, and $(C_M - C_o)$ of the order of 100, we find

$$\left(\frac{\Delta \varepsilon_T}{\varepsilon_T}\right)_{rnd} \approx \pm 1\%$$

As far as the systematic error on ε_T is concerned, we have taken the view of attributing the discrepancy between theoretical and experimental spectra to an actual energy degradation. If this were strictly true, our values for ε_T would only be affected by the random error. Since, however, the possibility of non-linearities or of a wrong estimate of the absolute position of C_o can not be entirely discarded, our values of ε_T could be affected by an error of approximately -4%. This last figure is a worst-case estimate.

The corresponding systematic error on L is -2.7% at 800 MeV and -2.3% at 1100 MeV.

a2) Error on Ω. -

The collimators defining our apertures have been positioned using the beam itself. Allowing for a ± 5 mm "random"(x) beam displacement, the corresponding error on L is $(0 \div +0.2)\%$ at 800 MeV.

Note that (see Ref. (1)), since our aperture is 6 mrad, L_{SB} is very insensitive to errors on the solid angle.

a3) Error on the correction for conversions in the thick window. -

As seen in § 6, our data have been corrected by the factor

$$f_{SB} = 1.133 \pm 0.005$$

on account of the conversions in the thick window. The corresponding error of $\pm 0.5\%$ has to be added to the other systematic errors.

b) - Double bremsstrahlung. -

The discussion just carried out on SB errors can be repeated for DB. Systematic errors on the thresholds are approximately the

---

(x) - Meaning that it could vary from one run to the next.

same for the two counters, so that errors on L are roughly just about twice those for SB. Taking the shapes of the spectra into account in some more detail (SW2 shows a slightly better agreement between theoretical and experimental distributions than SW1), the systematic error on L_{DB} can be estimated to be(x)

$$-3.4 \leq \frac{\Delta L_{DB}}{L_{DB}} \leq 0 \qquad \text{at} \quad 1.1 \text{ GeV}$$

$$-3.6 \leq \frac{\Delta L_{DB}}{L_{DB}} \leq 0 \qquad \text{at} \quad 0.8 \text{ GeV}$$

The random error on L_{DB} related to the evaluation of C_M, C_T, C_o is in this case $\pm$ 1%.

The solid angle, due to the different angular distribution of DB (see Ref. (1)), gives also rise to a larger systematic error, which can change from one run to the next. Under the same hypothesis already made for SB we find

$$\left(\frac{\Delta L_{DB}}{L_{DB}}\right)^{RND}_{\Omega} = + 0.5\%$$

Allowing for a $\pm$ 1% error ($\pm$ 6 cm) in the source-collimator distance, the corresponding systematic error on L_{DB} is

$$\left(\frac{\Delta L_{DB}}{L_{DB}}\right)^{SYST}_{\Omega} = \pm 0.2\%$$

The correction for the conversions in the thick window (see § 6) also introduces a systematic error

$$\left(\frac{\Delta L_{DB}}{L_{DB}}\right)^{SYST}_{f_{DB}} = \pm 1.2\%$$

(x) - $\frac{\Delta L}{L}$ is defined as $\frac{L_{True} - L_{Measured}}{L_{Measured}}$

C_T, C_o, C_M are affected both by random and by systematic errors. The random error on C_T, C_o and C_M is of the order of ± 0.1 channels at most. $(C_T - C_o)$ being of the order of 15, and $(C_M - C_o)$ of the order of 100, we find

$$\left(\frac{\Delta \varepsilon_T}{\varepsilon_T}\right)_{rnd} \approx \pm 1\%$$

As far as the systematic error on ε_T is concerned, we have taken the view of attributing the discrepancy between theoretical and experimental spectra to an actual energy degradation. If this were strictly true, our values for ε_T would only be affected by the random error. Since, however, the possibility of non-linearities or of a wrong estimate of the absolute position of C_o can not be entirely discarded, our values of ε_T could be affected by an error of approximately -4%. This last figure is a worst-case estimate.

The corresponding systematic error on L is -2.7% at 800 MeV and -2.3% at 1100 MeV.

a2) Error on Ω. -

The collimators defining our apertures have been positioned using the beam itself. Allowing for a ± 5 mm "random"(x) beam displacement, the corresponding error on L is $(0 \div +0.2)\%$ at 800 MeV.

Note that (see Ref. (1)), since our aperture is 6 mrad, L_{SB} is very insensitive to errors on the solid angle.

a3) Error on the correction for conversions in the thick window. -

As seen in § 6, our data have been corrected by the factor

$$f_{SB} = 1.133 \pm 0.005$$

on account of the conversions in the thick window. The corresponding error of $\pm 0.5\%$ has to be added to the other systematic errors.

b) - Double bremsstrahlung. -

The discussion just carried out on SB errors can be repeated for DB. Systematic errors on the thresholds are approximately the

---

(x) - Meaning that it could vary from one run to the next.

same for the two counters, so that errors on L are roughly just about twice those for SB. Taking the shapes of the spectra into account in some more detail (SW2 shows a slightly better agreement between theoretical and experimental distributions than SW1), the systematic error on L_{DB} can be estimated to be(x)

$$-3.4 \leq \frac{\Delta L_{DB}}{L_{DB}} \leq 0 \qquad \text{at} \quad 1.1 \text{ GeV}$$

$$-3.6 \leq \frac{\Delta L_{DB}}{L_{DB}} \leq 0 \qquad \text{at} \quad 0.8 \text{ GeV}$$

The random error on L_{DB} related to the evaluation of C_M, C_T, C_o is in this case $\pm$ 1%.

The solid angle, due to the different angular distribution of DB (see Ref. (1)), gives also rise to a larger systematic error, which can change from one run to the next. Under the same hypothesis already made for SB we find

$$\left(\frac{\Delta L_{DB}}{L_{DB}}\right)^{RND}_{\Omega} = +0.5\%$$

Allowing for a $\pm$ 1% error ($\pm$ 6 cm) in the source-collimator distance, the corresponding systematic error on L_{DB} is

$$\left(\frac{\Delta L_{DB}}{L_{DB}}\right)^{SYST}_{\Omega} = \pm 0.2\%$$

The correction for the conversions in the thick window (see § 6) also introduces a systematic error

$$\left(\frac{\Delta L_{DB}}{L_{DB}}\right)^{SYST}_{f_{DB}} = \pm 1.2\%$$

(x) - $\frac{\Delta L}{L}$ is defined as $\frac{L_{True} - L_{Measured}}{L_{Measured}}$

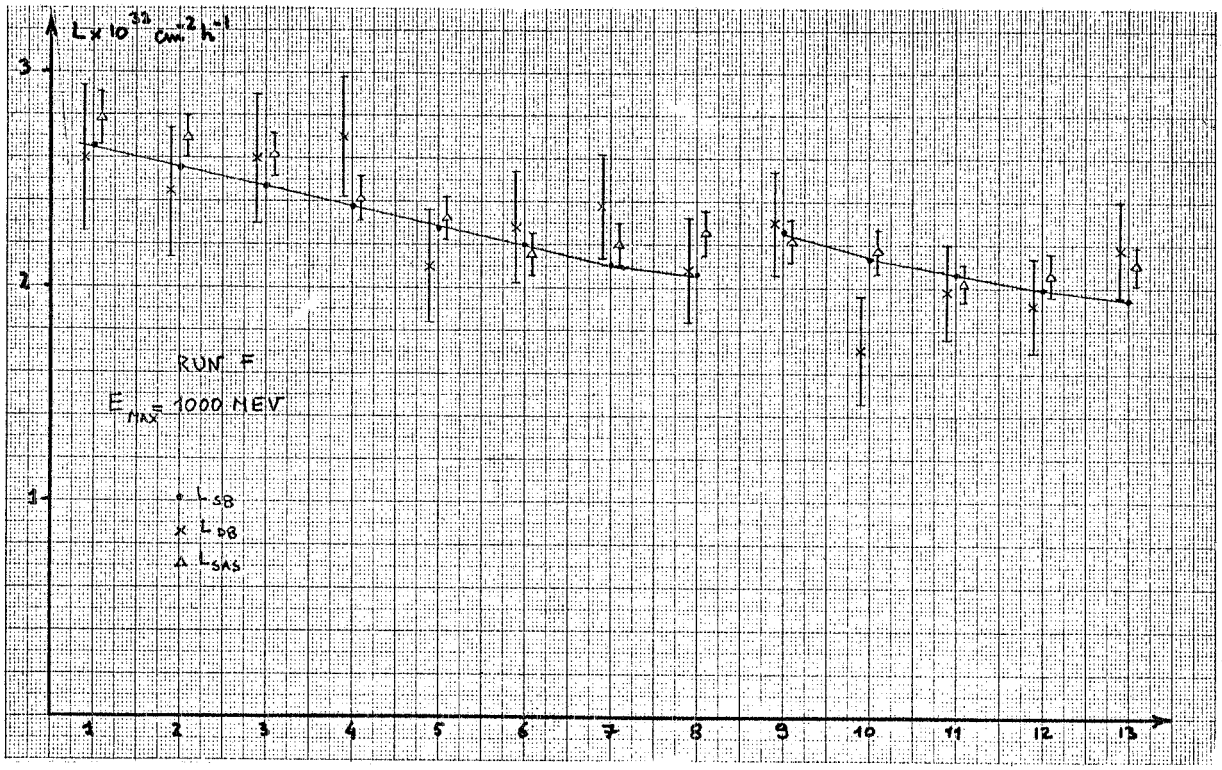

FIG. 14 - Typical luminosity measurement run - Experimental points refer to 1000 sec measurements. Beam energy 1000 MeV.

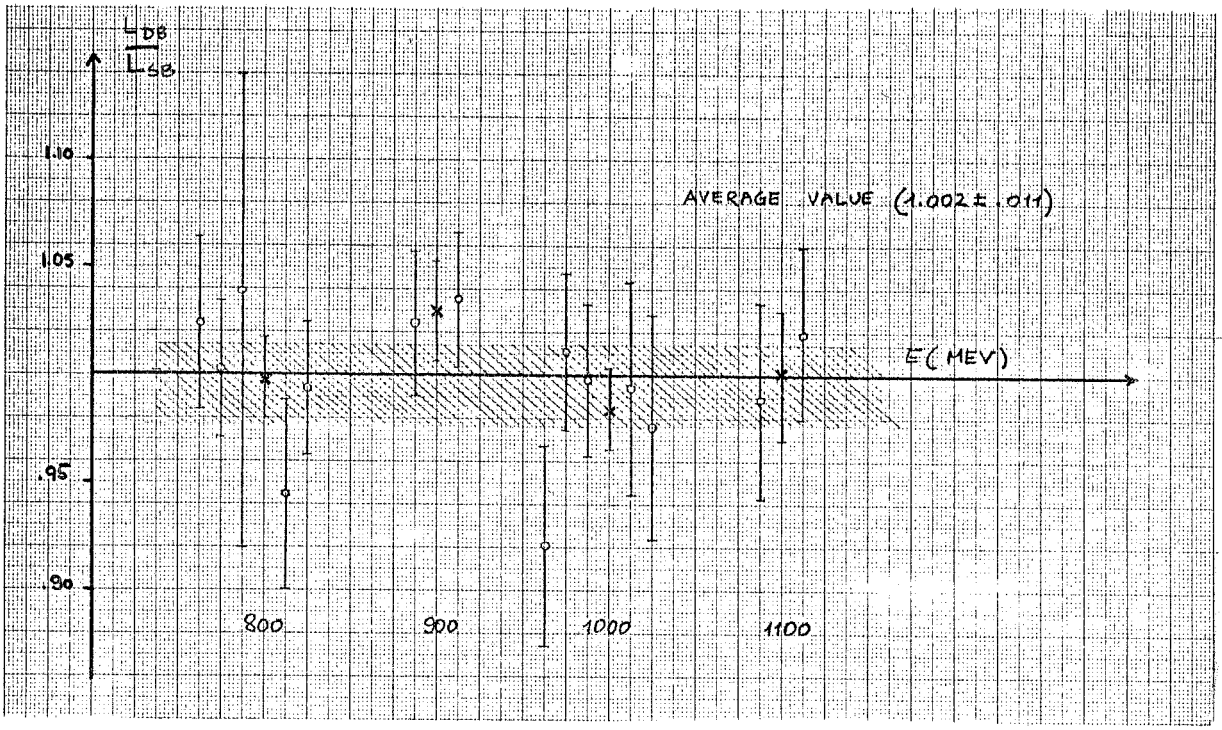

FIG. 15 - Values of L_{DB}/L_{SB}. Crosses are the average values of the points at the same energy.

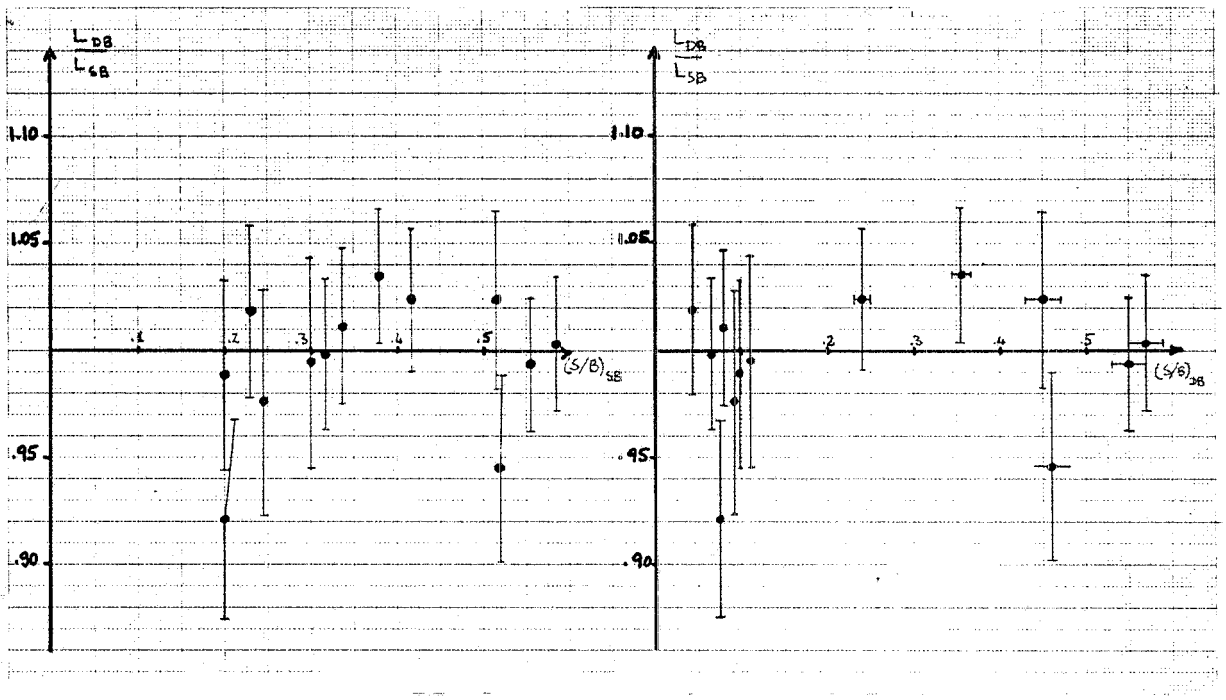

FIG. 16 - L_{DB}/L_{SB} as a function of signal-to-background ratio. Single and double bremsstrahlung.

machine is operating with head-on collisions). The main machine parameters involved are RF voltages, phases and frequency. These parameters can, to some extent, change from one run to the next, entraining a corresponding variation in the systematic errors on SAS luminosity. The small-angle-scattering cross section also depends on the absolute value of the beam energy. The distribution of the points around their average value is not quite statistical ($\chi^2/N \approx 3$), reflecting the fact that individual runs may be affected by different systematic errors.

The "average" deviation of the points from $L_{SAS}/L_{SB} = 1$ is $(4.5 \pm 0.5)\%$(x). The systematic errors on SB measurements are given in § 2, and the systematic errors on SAS are of the same order (see Reference (6)) of the above mentioned "average" deviation on the ratio L_{SAS}/L_{SB}. The two measurements are therefore compatible with each other, within the expected systematic errors.

(x) - The SAS data we have used were analyzed by F. Ceradini of the "$\mu - \pi$" group.

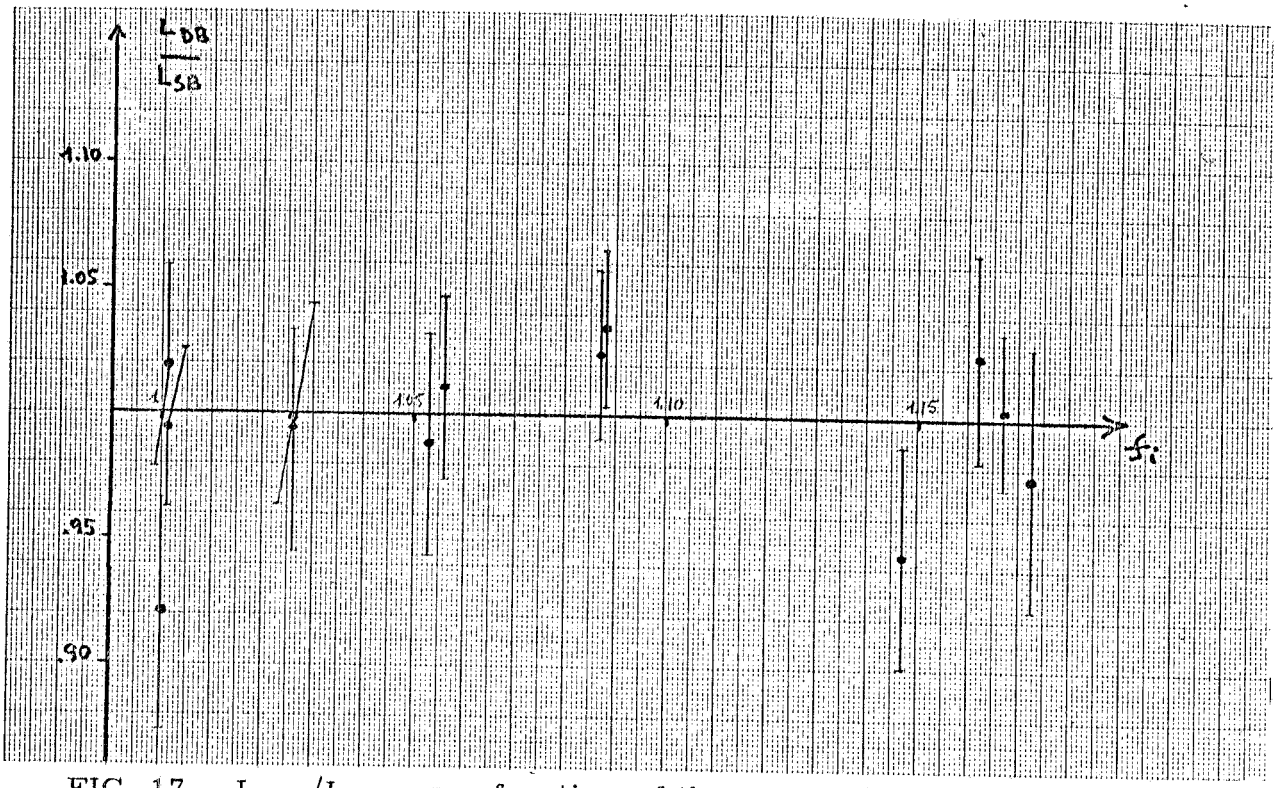

FIG. 17 - L_{DB}/L_{SB} as a function of the correction for the residual e^- bunch.

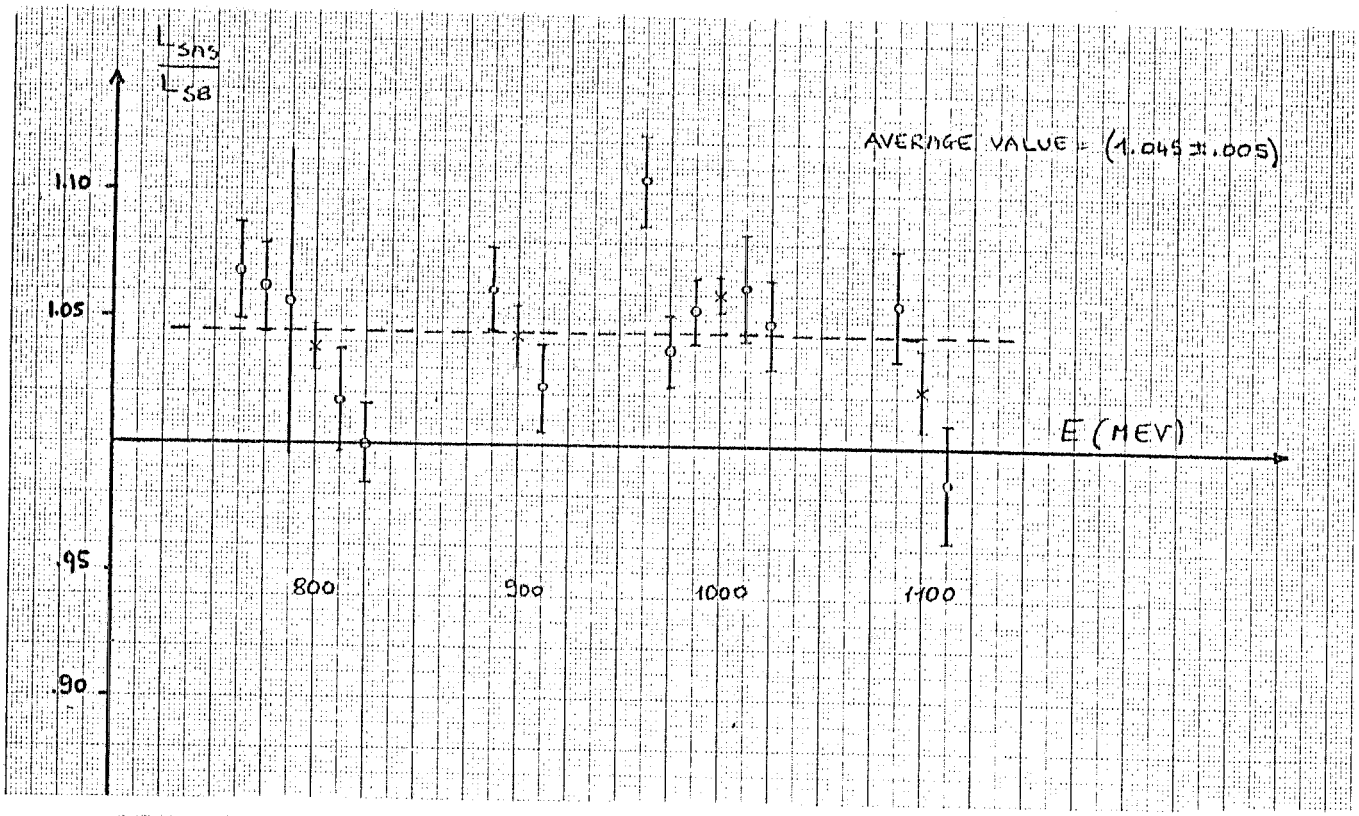

FIG. 18 - Values of L_{SAS}/L_{SB}. Crosses are the average values of the points at the same energy.

ACKNOWLEDGEMENTS. -

We thank all the physicists and technicians (see Ref. (4)) who have designed, built and operated the SAS monitoring system and in particular: F. Ceradini for collaborating during the runs and for providing us with the SAS data, and G. Nicoletti for constant technical assistance.

We are very grateful to all our colleagues of the Adone group for support and discussions, and in particular to M. Placidi and M. Vescovi for taking active part in collecting the data and for running the machine to our requirements.

REFERENCES. -

(1) - S. Tazzari, Considerations on a luminosity monitor at Adone, LNF-67/23 (1967).
(2) - E. Segrè, Experimental Nuclear Physics, p. 260.
(3) - H. W. Koch and J. W. Motz, Bremsstrahlung cross sections and related data, Revs. Modern Phys. 31, 920 (1959).
(4) - G. Barbiellini, B. Borgia, M. Conversi e R. Santonico, Atti della Accademia Nazionale dei Lincei 44, 233 (1968); R. Santonico, Thesis, University of Rome; M. Preger, Thesis, University of Rome.
(5) - H. C. Dehne and M. Preger, Numerical calculations on the small angle scattering luminosity monitor used at Adone, LNF-70/33 (1970).
(6) - G. Barbiellini et al., Luminosity measurement at Adone by small angle Bhabha scattering, To be published.